

Novel Tools and Methods

Development of Eight Wireless Automated Cages System with Two Lickometers Each for Rodents

Mariana Cardoso Melo, Paulo Eduardo Alves,  Marianna Nogueira Cecyn, Paula Mendonça C. Eduardo, and Karina P. Abrahao

<https://doi.org/10.1523/ENEURO.0526-21.2022>

Departamento de Psicobiologia, Escola Paulista de Medicina, Universidade Federal de São Paulo (Unifesp), São Paulo, Brazil

Abstract

Drinking behavior has been used in fundamental research to study metabolism, motivation, decision-making and different aspects of health problems, such as anhedonia and alcohol use disorders. In the majority of studies, liquid intake is measured by weighing the bottles before and after the experiment. This method does not tell much about the drinking microstructure, e.g., licking bouts and periods of preference for each liquid, which could be valuable to understand drinking behavior. To improve data acquisition of drinking microstructure, companies have developed lickometer devices that acquire timestamps when animals approach or drink from a specific sipper. Nevertheless, commercially available devices have elevated costs. Here, we present a low-cost alternative for a lickometer system that allows wireless data acquisition of licks from eight cages with two sippers each. We ran a three-phase validation protocol to ensure (1) proper choice of the sensor to detect licks; (2) adaptation of the device to a wireless transmission and realistic *in silico* tests; and (3) *in vivo* validation to test the correlation between the amount of licks measured by the lickometer and the bottle weight. The capacitive sensor presented appropriate recall and precision for our device. After adaptation to wireless transmission, the *in silico* validation demonstrated low reading and transmission errors even when tested in extreme simultaneous licking conditions. Finally, we observed a positive correlation between water or ethanol consumption and lick count, showing that the lickometers can be used for *in vivo* studies interested in rodent drinking microstructure.

Key words: behavior; drinking microstructure; lickometer; mice; prototype validation; two-bottle choice

Significance Statement

This study presents an innovative and low-cost solution for drinking behavioral studies: a lickometer system based on an open-source hardware platform with a user-friendly interface software, capable of simultaneously receiving data from eight automated cages with two drinking bottles each. The lickometer brings an accessible device to acquire high-quality and detailed data. This device also has the possibility to be adaptable to new types of sensors or other neuroscience tools capable of measuring brain activity simultaneously to the behavior.

Introduction

Liquid intake is an essential animal behavior. Together with feeding and sexual behavior, drinking water (or other liquids) is influenced by genetic and environmental factors (Ramirez and Sprott, 1978; Bachmanov et al., 2002; Bainier et al., 2017). Scientists have been using

drinking behavior in rodents to study metabolism, motivation, decision-making, and different aspects of psychological and medical problems, such as alcohol use disorders (Jeanblanc et al., 2019). Sometimes, animals are exposed to more than one drinking bottle containing

Received December 7, 2021; accepted July 11, 2022; First published July 18, 2022.

The authors declare no competing financial interests.

Author contributions: M.C.M. and K.P.A. designed research; M.C.M., P.E.A., M.N.C., P.M.C.E., and K.P.A. performed research; K.P.A. contributed unpublished reagents/analytic tools; M.C.M., P.E.A., and K.P.A. analyzed data; M.C.M., M.N.C., P.M.C.E., and K.P.A. wrote the paper.

different liquids and have to decide what to drink. This protocol has often been called the two-bottle choice model (Barkley-Levenson and Crabbe, 2015; Panksepp et al., 2017). In these studies, the volume consumed is recorded usually by weighing bottles before and after animals drink from them.

Although these studies have produced valuable data for different fields of psychobiology, there is greater complexity in drinking behavior. Drinking is highly influenced by light/dark circadian rhythms (Eisenhardt et al., 2015; Bainier et al., 2017; Gamsby et al., 2017), indicating that measures of drinking in different periods can reveal different results. In addition, different drinking patterns can produce interesting interpretations of the data, even when the total volume consumed is similar. In humans, for example, researchers have studied the microstructure of sucrose intake to detect different motivational states (Gero et al., 2019). Differences in drinking initiation, bout duration, and timing may indicate compulsive-like states in rodents, as specific drinking behavioral characteristics are observed in ethanol aversion-resistant intake protocol (Darevsky et al., 2019; Darevsky and Hopf, 2020). Thus, collecting detailed data is an important step for further evaluation of this type of behavior.

In order to study drinking microstructure, scientists have been using automated lickometers (Barkley-Levenson and Crabbe, 2015; Cains et al., 2017; Frie and Khokhar, 2019; Godynnyuk et al., 2019). These devices can collect timestamps every time animals approach or drink from a specific sipper. However, many commercially available lickometers are extremely costly for laboratories. Alternatively, low-cost and open-source devices have been found in the literature, created with electronic code prototyping platforms (Longley et al., 2017; Frie and Khokhar, 2019; Godynnyuk et al., 2019). There are at least two types of these devices: photoelectric/barrier sensor-based (Frie and Khokhar, 2019) or capacitive sensor-based (Longley et al., 2017). In both cases they are designed to have one circuit board for two bottles on each animal cage. If the behavioral experiment requires a significant number of animals, specific cages for each rodent could imply great development efforts. Furthermore, most of the validation procedures use only correlation analysis between the animal's sipper interactions and bottle weight or

preference for two types of liquids, such as water and sucrose (Longley et al., 2017; Godynnyuk et al., 2019).

The present work focused on developing an innovative and low-cost solution for drinking behavioral studies where it is necessary to run groups of animals at the same time. We propose a system capable of simultaneously receiving data from eight automated cages with two drinking bottles each, using a wireless system. Our lickometer device enhances the experiment's robustness by collecting synchronized information from rodent behavior experiments. To reach the final system, we present in this paper three development and validation steps as the following: (1) selection of the proper licking detection sensor; (2) translation to wireless transmission and validation with emulated signals; and (3) *in vivo* validation using mice drinking in two-bottle lickometer cages.

Materials and Methods

Selection of the proper licking detection method

System description

We developed three prototypes with the respective types of sensors: light-dependent resistor (LDR), photoelectric, and capacitive (touch), as shown in Figure 1A (electronic schematic diagram of the three prototypes is presented in Extended Data Fig. 1-1). All prototypes consisted of an Arduino MEGA, used for the analog/digital conversion (A/D converter) of the sensor's signal, a Secure Digital (SD) card module to store the data, a real-time clock module (DS3231) to precisely time the licks events and a Liquid Crystal Display (LCD) 16 × 2 to show the number of licks and date/time of occurrence.

The licking apparatus was adapted according to the specificity of each sensor (Fig. 1B–D). One hole aligned to the bottle nozzle was made for the LDR sensor positioning (Fig. 1B). If the mice approached the cabin, the change in the luminosity altered the resistance of the LDR and, consequently, its voltage. The LDR prototype counted a new lick when a voltage threshold was reached. The photoelectric sensor was adjusted in two aligned holes in the opposite walls of the cabin (Fig. 1C). One hole corresponded to the photoelectric emitter and the other to the photoreceiver. Thus, in this case, the lick count occurred when the animal interrupted the signal between emitter and receiver. Finally, the capacitive sensor prototype required an adaptation of the house cage to weld a 65-mm stainless steel to the sipper and connect it to the Arduino's analog input. Also, an aluminum platform was installed in the cage to create the system ground when mice step on top of it (Fig. 1D). In order to turn the Arduino pin, connected to the steel bottle nozzle, into a capacitive sensor we used the library *CapacitiveSensor* (Bagder, 2015). A lick was counted when the mice simultaneously touched the bottle nozzle and the aluminum platform.

Animals

The animal experiments were approved by the Comissão de Ética em Uso de Animais (CEUA), Universidade Federal de São Paulo (#1482300519). For prototype validation, we

This work was supported by the 2019 Return Home Fellowship from the International Brain Research Organization (IBRO), the Conselho Nacional de Desenvolvimento Científico e Tecnológico (CNPq) Grant #434092/2018-5, and the São Paulo Research Foundation (FAPESP) Student Fellowship #2019/24650-0 and Grant #2019/01686-0.

Acknowledgments: We thank the staff of the Departamento de Psicobiologia, Universidade Federal de São Paulo (UNIFESP), and the Associação Fundo Incentivo à Pesquisa (AFIP) for the infrastructure support for this work. We also thank Fernando Bezerra for the help with video analysis.

Correspondence should be addressed to Karina Possa Abrahao at kabrahao@unifesp.br.

<https://doi.org/10.1523/ENEURO.0526-21.2022>

Copyright © 2022 Cardoso Melo et al.

This is an open-access article distributed under the terms of the Creative Commons Attribution 4.0 International license, which permits unrestricted use, distribution and reproduction in any medium provided that the original work is properly attributed.

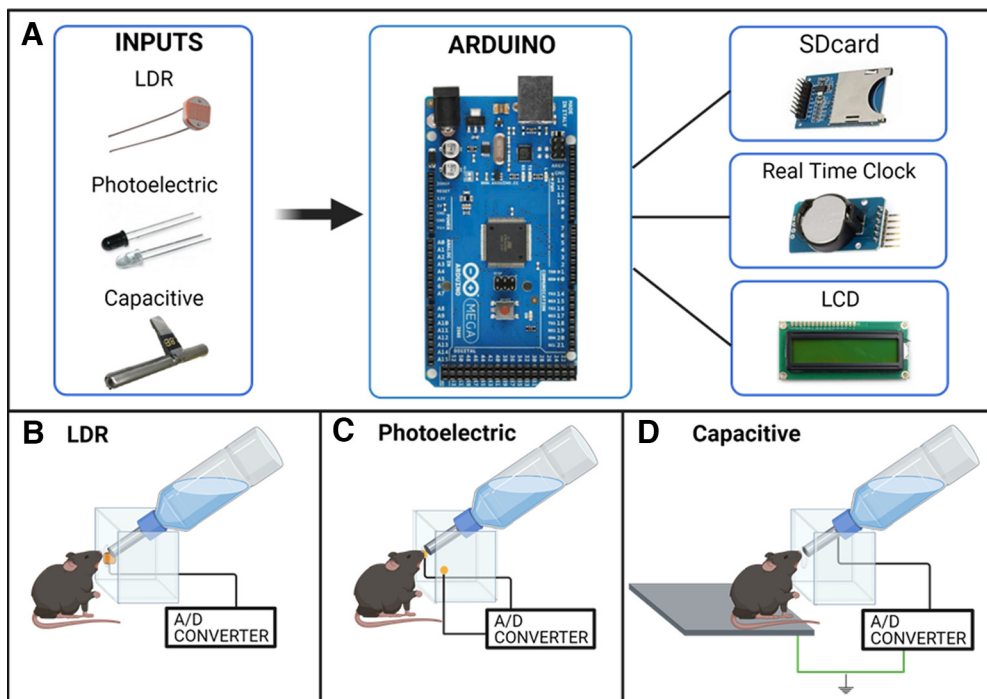


Figure 1. Schematic illustration of prototypes. **A**, Electronic components, where the three selected sensors are shown in the INPUTS box: LDR, photograph emitter/photosensor (photoelectric), and the capacitive sensor (with a 65-mm stainless steel nozzle). An Arduino MEGA was used as an analog-digital signal converter. The shields are shown on the right: an SD card module to record the collected data, a real-time clock module (DS3231) and an LCD 16 × 2 to show, licks counting in real time. **B–D**, Prototypes' schematic showing the lick cabin for each sensor, the mouse positioning, the liquid bottle and the sensors. **B**, LDR prototype sensor was positioned at one side of the lick cabin. **C**, The photoelectric prototype sensor had the photo emitter aligned to the photoreceiver on the lick cabin. **D**, The capacitive prototype sensor was created by the connection between the stainless-steel nozzle to an analog input of the Arduino (black wire), and the platform was connected to the ground (Gnd, green wire). Created with BioRender. For electronic schematic diagram, please see Extended Data Figure 1-1.

used four C57Bl/6 mice (two females and two males; 30–90 days old at the beginning of experiments, from the Centro de Desenvolvimento de Modelos Experimentais para Medicina e Biologia - CEDEME). Animals were individually housed in ventilated racks and kept on a 12/12 h light/dark cycle (light onset at 7 a.m.) with *ad libitum* access to food and water.

Experimental procedure

Water and food were withdrawn from the mice's home cage 2 h before the test in order to increase motivation. We first acquired data from lickometer cages without the presence of a mouse, for 1 min to capture the sensor's baseline values. Mice were then individually placed in the experimental cage and a bottle with 5% sucralose solution was placed on the licking cabin for each prototype. Researchers observed whether the dimension and position of the drinking bottle were ergonomic for mice. We chose an ergonomic design to avoid mice having any kind of difficulty accessing the drinking sippers, in relation to the height (5 cm of the floor) and angle (60°) of the sipper. Additionally, the licking threshold (value above baseline considered a lick event) was estimated for each prototype by observing the sensor values when the animal approached or moved away from the bottle nozzle. Finally, we designed the initial validation experiment to compare the three prototypes as described below.

All mice were tested twice in each prototype. The experiments were recorded by a camera positioned to record the mouse's licks behavior and the LCD that exhibited the counts. Each experiment lasted as long as necessary for the prototypes to register at least 100 licks per mouse. The verification of a new lick occurred every 50 ms. A 5-ms delay after a licking event was used to ensure the system did not count duplicate licks whenever a lick detection occurred.

Four researchers watched all the videos. In order to visualize licks, the speed of the videos was slowed down to 0.25×. Researchers detected the presence of true positives, false positives or false negatives, and the time each lick occurred for each video. True positives were reported when an animal licked the sipper and the prototype correctly measured it; false positives, when the system accounted for a new lick but the animal did not do it; false negatives, when the animal did lick the sipper but the system did not count it. Two metrics, precision and recall, were estimated based on these values. Precision corresponds to the ratio of true positives among true and false positives, and recall corresponds to the ratio of true positives in relation to false negatives and true positives. Thus, precision informs the proportion of actual correct positive identification of licks and recall informs the proportion of actual positive lick counts identified correctly.

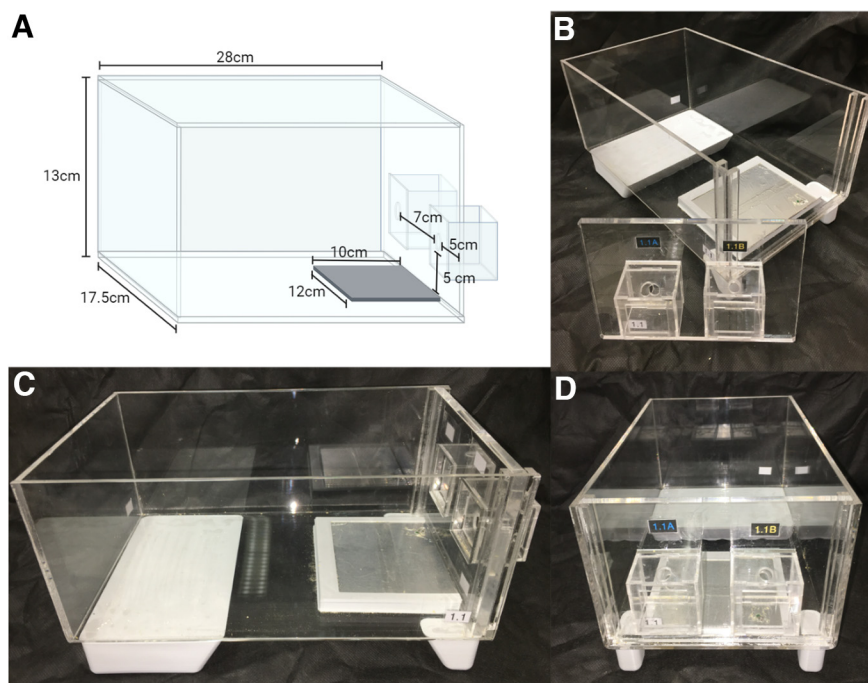


Figure 2. **A**, Designed acrylic cage dimensions for the lickometer. **B**, Removable wall with the cabins where drinking sippers are positioned. **C**, Lateral view. **D**, Front view.

Recall and precision data were compared between prototypes by an independent t test (GraphPad Prism), with a level of significance of $p < 0.05$.

Translation to wireless transmission and *in silico* validation with emulated signals

System description

Based on the sensor's selection with greater precision and recall obtained in the first stage of validation, eight house cages were adapted to have two bottle-coupled sensors.

Acrylic cages were designed to support two drinking sippers. Its dimensions can be seen in Figure 2A. Also, the support for the drinking sippers was planned to be removable (Fig. 2B), allowing scientists to remove it in a way to help maintenance and cleaning of the cage. We also developed an electronic circuit to acquire the signals from eight cages, using 95% insulated cables, and send them wirelessly to a desktop computer (Fig. 3). A real-time clock module was used to timestamp the precise time of each lick. As the ESP8266 NodeMCU module has only one analog input, a 16-channel multiplexer was used to receive the corresponding signals from all sensors of the

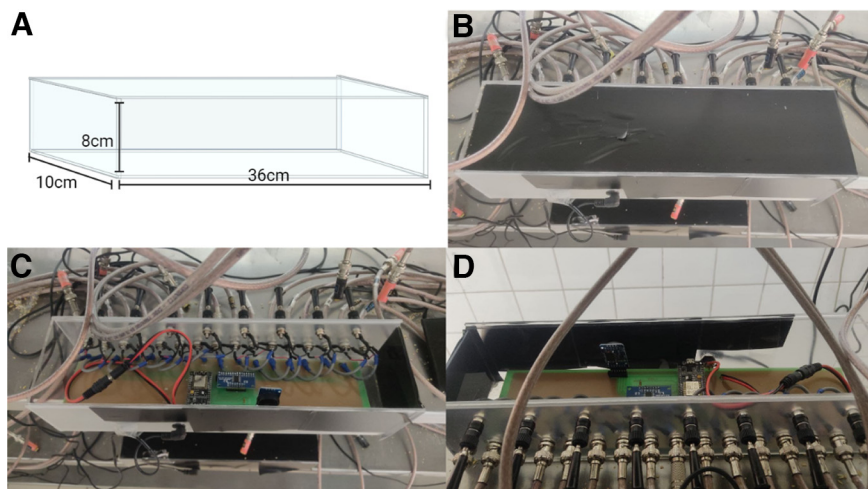


Figure 3. **A**, Acrylic box designed to store the electronic circuit. **B**, Top view. **C**, Top view of the open circuit box. **D**, Front view shows the cables that connect the sensors with the electronic circuit.

Table 1: List of materials used to build the full system of eight house cages and the components of the electronic central unit

Materials	Quantity	Unit cost	Total cost	Estimated total cost (US\$)
ESP8266	1	R\$ 30.00	R\$ 30.00	US\$ 6.00
Module RTC	1	R\$ 25.00	R\$ 25.00	US\$ 5.00
Module Mux 74 hc4067	1	R\$ 15.00	R\$ 15.00	US\$ 3.00
Pin bar 1 × 40	6	R\$ 1,50	R\$ 9.00	US\$ 1.80
Switched mode power supply 5V 1A	1	R\$ 12.00	R\$ 12.00	US\$ 2.40
PowerSupply connector/jack P4 female 5.5 x 2.1 mm	1	R\$ 0.60	R\$ 0.60	US\$ 0.12
Female BNC connectors	32	R\$ 2.20	R\$ 70.40	US\$ 14.08
Male BNC connector RG59 75R	32	R\$ 4.80	R\$ 153.60	US\$ 30.72
Coax cable RG59 750HM 96%	16	R\$ 3.00	R\$ 48.00	US\$ 9.60
Banana jack 4 mm	8	R\$ 1.30	R\$ 10.40	US\$ 2.08
Cable 0.25 mm	8	R\$ 1.00	R\$ 8.00	US\$ 1.60
Female pin B67	8	R\$ 7.00	R\$ 56.00	US\$ 11.20
Male pin P22	8	R\$ 0.16	R\$ 1.28	US\$ 0.26
FBU 323101 terminal	16	R\$ 0.30	R\$ 4.80	US\$ 0.96
Resistor 100K	2	R\$ 0.05	R\$ 0,10	US\$ 0.02
General expenses (glue, resin...)	1	R\$ 100.00	R\$ 100.00	US\$ 20.00
Printed circuit board for grounding	8	R\$ 30.00	R\$ 240.00	US\$ 48.00
Printed circuit board for wireless central	1	R\$ 48.68	R\$ 48.68	US\$ 9.74
Acrylic box for circuit	1	R\$ 200.00	R\$ 200.00	US\$ 40.00
Acrylic cage	8	R\$ 220.00	R\$ 1760.00	US\$ 352.00
Welding the nozzle to the connector	16	R\$ 20.00	R\$ 36.00	US\$ 7.20
Total cost			R\$ 2828.86	US\$ 565.78

The values were considered with the Brazilian currency (real, R\$) in February 2021 and converted to the United States dollar. The dollar exchange rate was considered on February 23, 2022.

lickometers. Then, the transmission circuit sent all data wirelessly to a computer, with the User Datagram Protocol (UDP), through a NodeMCU ESP8266 module.

In order to acquire the typical lick interval of mice and allow the wireless transmission of the data, we set a sampling rate of 60 ms, which is an appropriate sampling rate for measuring licking behavior. According to Boughter et al. (2007), the average licking rate of a C57Bl/6 mouse is 8.5 licks/s, thus the proposed system acquires 16.67 samples per second which is appropriate to detect lick samples.

We also built a protocol to simulate licks *in silico* which allowed us to verify the efficacy of the proposed wireless system. A potentiometer was used as an on/off switch (“on” or “high-level” means a lick; “off” means no-lick). First, we considered a situation where only one mouse in one lickometer cage would lick one sipper. Next, we increased the number of cages in this condition until a situation in which animals in all eight lickometer cages would lick at the same time. Considering the mean licking rate for mice ranges between 6 and 9 Hz (Boughter et al., 2007; Rossi et al., 2016; Williams et al., 2018), we decided to simulate licks representing low and high-frequency situations. Thus, signals were emitted through the digital ports of the microcontroller ESP8266 at frequencies of 5 and 10 Hz, which allowed a minimum interlick interval (ILI) detection of 200 and 100 ms, respectively. The 5 Hz frequency (ILI = 200 ms) was selected to simulate a typical licking rate, so we could verify how our system responds in ordinary situations. Tests performed at 10 Hz represent a scenario where all eight animals would be licking simultaneously at a higher frequency (ILI = 100 ms).

Table 1 lists the electronic components of one lickometer system and the costs in real (Brazilian currency) and estimated cost in US dollars.

Experimental procedure

In total, we have built three sets of eight cages. Each cage had two bottles with sensors that we referred to as A (output A) and B (output B). The *in silico* validation consisted of three phases (Fig. 4). First, emulated lick signals were sent only from output A (Phase 1); then, only from the output B (Phase 2); finally, in the last phase (Phase 3), the signals were sent alternately to each output of the same cage. For each phase, the system sent twelve thousand high-level signals. The number of cages simultaneously receiving the emulated signals increased in each trial. This means that only one sensor of one cage received high-level signals, then only one sensor of two cages received high-level signals simultaneously, and so on, until one sensor of eight cages received simultaneous signals. The same was repeated to the other sensor in the same cages in Phase 2 and alternated for each lickometer in each cage in Phase 3. With the incremental number of cages, it was possible to verify whether the error is correlated with the number of sensors.

We analyzed two types of errors: the reading error (percentage of times the central system did not recognize the licking event correctly before sending it wirelessly to the computer) and the transmission error (the loss of data during transmission via UDP). Both errors were measured for high and low frequency (5 and 10 Hz, respectively). The statistical differences of the reading or transmission errors were compared considering different phases, frequencies and number of cages according to the data normality test. A level of 5% was considered significant, and a Bonferroni *post hoc* was used when necessary.

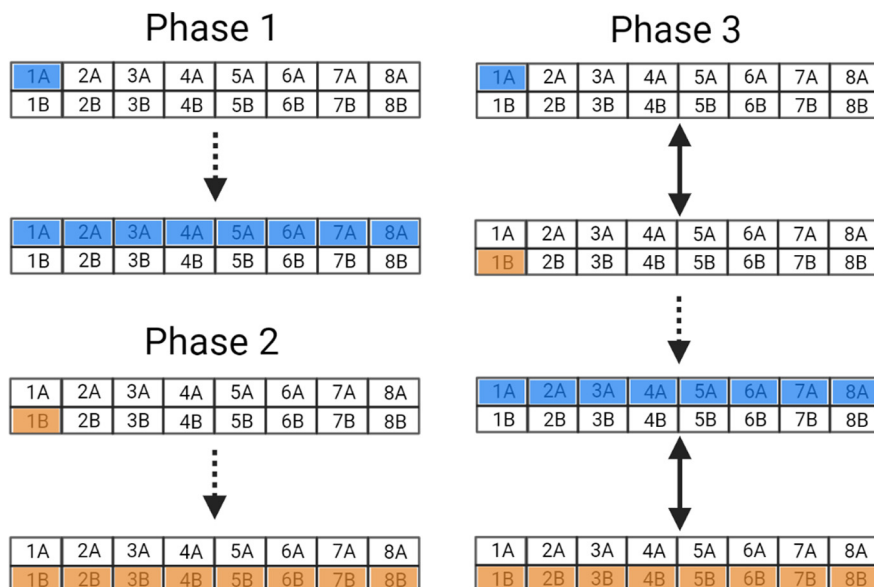


Figure 4. Experimental design of the *in silico* validation protocol with emulated signals. Digital pulses emulating licks were emitted through the digital ports of the microcontroller ESP8266 at frequencies of 5 and 10 Hz. In total, we have built eight cages, each cage has two bottles with sensors that we referred to as A and B. The validation consisted of three phases, in which the number of licks was simulated by alternating each bottle. Phase 1: the pulses initially were sent only from one output A (blue square) to simulate licks from the lickometer A (blue) of one house cage, then two A outputs until simultaneously eight outputs were sending pulses from lickometers A to simulate simultaneous licks from the eight house cages on the lickometers A of each cage. Phase 2: the signals were sent only from the sensor connected to the lickometer B (orange), repeating Phase 1 for this output. Phase 3: pulses were sent from both lickometers A and B, alternately. Thus, signals were sent from one output A (blue) followed by one output B (orange) until simultaneously eight house cages send A and B signals. Created with BioRender.

In vivo validation

System description

The last validation step of our system consisted of testing the system with animals individually housed in the lickometer cages to verify the correlation between drinking and licks count registered by the system. We have built three lickometer systems which allowed us to record from 24 cages and 48 lickometers at the same time (one system is shown in Fig. 5). A software in C# was developed to allow acquisition of wireless data and its visualization, including baseline noise and licks as well as to store the sensor raw input data at 16.67 Hz in a text file. Data were then analyzed in MATLAB in which an appropriate licking threshold was established.

Animals

The experiments were approved by the CEUA, Unifesp (#5327090819). We used C57Bl/6 mice (24 males and 24 females; seven weeks old at the beginning of experiments, from the CEDEME), housed in two to four animals per home cage in ventilated racks and kept on a 12/12 h light/dark cycle (light onset at 7 a.m.) with *ad libitum* access to food and water.

Experimental procedure

In order to observe whether the system could quantify licks that can indicate the amount of liquid drunk overnight, one bottle was filled with water and the other was filled with 10% v/v ethanol (C57Bl/6 mice tend to drink high amounts of ethanol). We used an intermittent overnight

drinking protocol, in which mice were placed in the lickometer cages 2 h before the lights went off for 16 h, every other night, three nights per week for four weeks. The bottles were weighed before and after each drinking night. We ran two iterations of this experiment with 24 animals in each. Spearman correlations between the total fluid intake (measured by the bottle weights in grams, before and after the overnight test) and the total amount of licks were determined using GraphPad Prism. A level of 0.05 was considered significant.

Results

Selection of the proper licking detection method

The LDR prototype was discarded since it did not present adequate stability in the preliminary experiments because of the impact of the environmental luminosity on the data acquisition. We used precision and recall data to compare the capacitive and the photoelectric prototypes (Fig. 6A). The capacitive prototype presented significantly higher precision (capacitive: $91.14 \pm 5\%$; photoelectric: $77.02 \pm 11.69\%$; mean \pm SD) when compared with the photoelectric prototype (unpaired *t* test; $t_{(54)} = 3.46$; $p = 0.01$; effect size Cohen's $d = 0.93$; Fig. 6B,D). The prototypes did not statistically differ for recall (capacitive: $90.79 \pm 4.62\%$; photoelectric: $93.56 \pm 8.98\%$; unpaired *t* test; $t_{(54)} = 0.98$; Fig. 6C,D). Thus, the capacitive prototype was selected for the next development and validation steps.

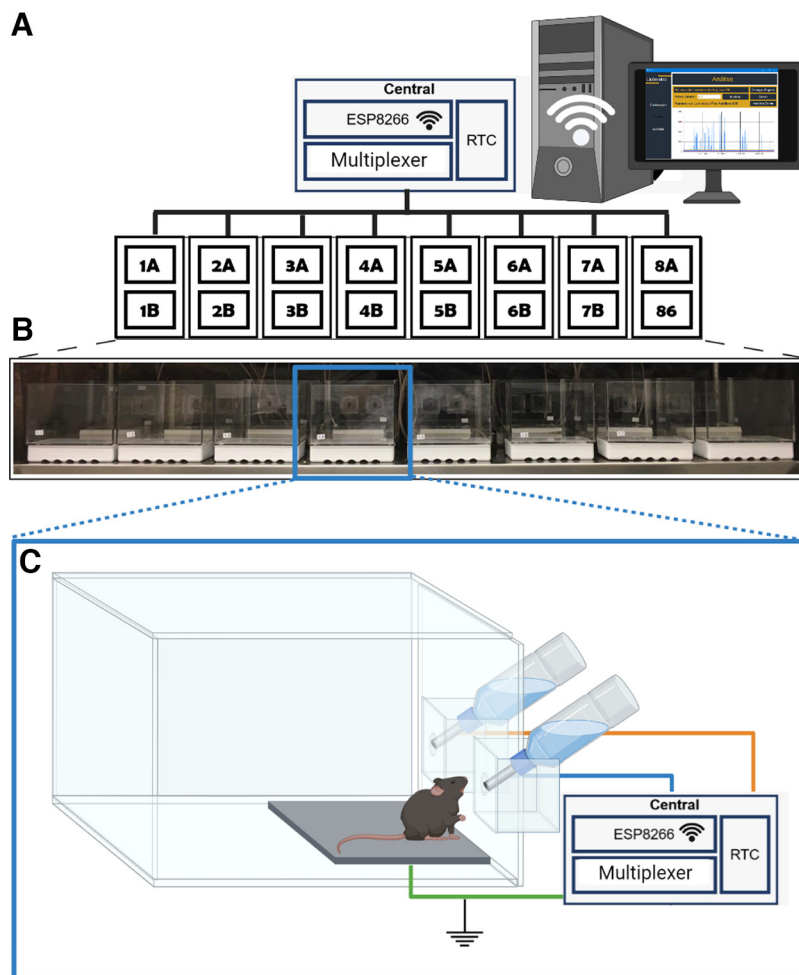


Figure 5. Illustration of one set of lickometer house cages with a detailed view of its parts. **A**, Schematic of the central system that transmits data from the sensors to the computer wirelessly. The central system consists of an ESP8266, a real-time clock (RTC) and a multiplexer. One central is connected to 16 lickometers from eight boxes. **B**, One actual set of eight house cages. **C**, Draft of the final house cage highlighting its parts. Both stainless steel nozzles are connected to an input of the central system (A: lickometer with blue wire and B: lickometer with orange wire), and the platform is connected to the ground (green wire). Created with BioRender.

Translation to wireless transmission and *in silico* validation with emulated signals

We adapted the initial capacitive prototype and translated the data transmission to a wireless protocol. Three sets of eight cages were built, with two lickometers (capacitive sensors) each. The central unit was used for the *in silico* validation of emulated signals. Figure 7 shows the results of the three simulation phases and their corresponding reading and transmission errors. Since the proposed validation phases in the same frequency required similar hardware capacity, we expected nondivergent transmission and read errors between phases.

Statistical tests were conducted to compare the reading error in different phases at different emulation frequencies considering different output signals (output A, Phase 1 or output B, Phase 2 or both outputs A and B, Phase 3). One independent-samples Kruskal–Wallis test was conducted for all reading error data to compare error among the different phases ($H_{(5)} = 60.035$; $p < 0.001$; $\eta^2 = 0.063$). The *post hoc* analysis revealed that the reading error (Fig. 7A–C) in Phase 1 at 5 Hz was lower than in

Phase 3 at 10 Hz ($p = 0.003$). Phase 2 at 5 Hz had a lower reading error than Phase 1 at 10 Hz ($p < 0.001$), Phase 2 at 10 Hz ($p < 0.001$), Phase 3 at 10 Hz ($p < 0.001$) and Phase 3 at 5 Hz ($p = 0.033$). In addition, Phase 3 at 5 Hz had lower reading error than Phase 3 at 10 Hz ($p < 0.001$). Another independent-samples Kruskal–Wallis test was conducted for all transmission error data ($H_{(5)} = 45.259$; $p < 0.001$; $\eta^2 = 0.068$). The *post hoc* analysis revealed that Phase 1 at 10 Hz had lower transmission error than Phase 2 at 5 Hz ($p < 0.001$) and 10 Hz ($p < 0.001$), as well as than Phase 3 at 5 Hz ($p < 0.001$) and Phase 3 at 10 Hz ($p = 0.016$). Phase 1 at 5 Hz had significantly lower transmission error than Phase 2 at 5 Hz ($p = 0.015$) and than Phase 3 at 5 Hz ($p = 0.03$).

Specific differences within the same frequency and phase among different number of cages (or channels) are represented in Figure 7 and were analyzed by a separate independent-samples Kruskal–Wallis test each. The *post hoc* results are represented in the graph by horizontal lines. No difference in reading error and number of cages was observed in Phase 1 at 5 Hz ($H_{(7)} = 9.904$; $p = 0.194$;

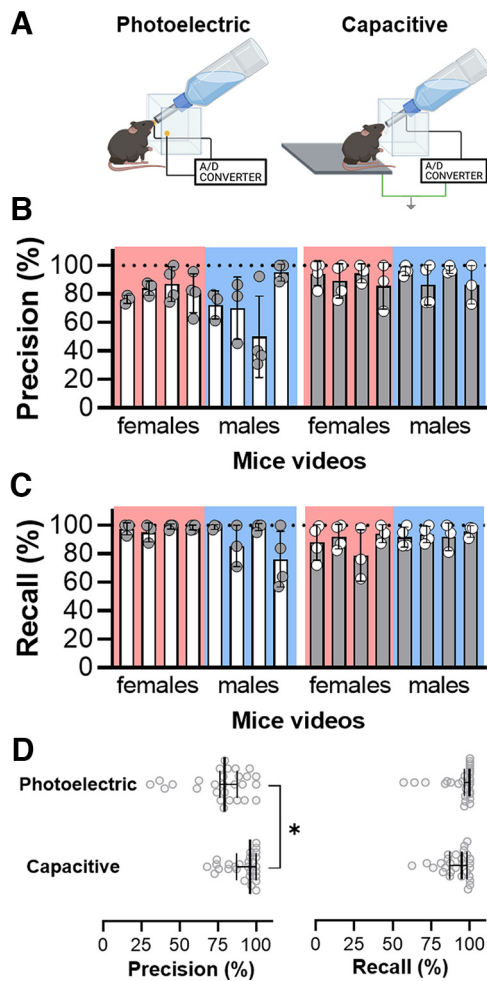


Figure 6. Results of recall and precision values for two prototypes. **A**, Diagram of the selected prototypes for validation: capacitive and photoelectric sensors connected to the Analog/Digital (A/D) converter. **B**, Descriptive results of the precision of the photoelectric and capacitive prototypes validation for female and male mice. Each graphical bar is the mean \pm standard deviation of the video evaluated by different researchers. **C**, Descriptive results of the recall of the photoelectric and capacitive prototypes validation for female and male mice. Each graphical bar is the mean \pm standard deviation of the video evaluated by different researchers. **D**, Graphical visualization of results of recall and precision for capacitive and photoelectric prototypes (median \pm 95% confidence interval). An independent *t* test detected a significant difference in precision between prototypes ($*p < 0.05$), being higher with slower dispersion for the capacitive sensor. Recall remained similar for both prototypes, without significant differences.

$\eta^2 = 0.087$), but the analysis detected significant differences at 10 Hz ($H_{(7)} = 14.834$; $p = 0.038$; $\eta^2 = 0.122$; Fig. 7A), although no specific difference among channels were detected by the *post hoc* analysis. For output B, Phase 2, the analysis detected significant differences for both emulated frequencies, 5 Hz ($H_{(7)} = 15.394$; $p < 0.001$; $\eta^2 = 0.08$) and 10 Hz ($H_{(7)} = 16.134$; $p < 0.001$; $\eta^2 = 0.144$; Fig. 7B). In both cases, no specific difference was detected by the *post hoc* analysis. In Phase 3, considering both outputs, the analysis detected significant differences at 5 Hz

($H_{(7)} = 16.941$; $p = 0.018$; $\eta^2 = 0.146$) and at 10 Hz ($H_{(7)} = 18.247$; $p = 0.011$; $\eta^2 = 0.178$; Fig. 7C).

The analysis detected significant differences for the transmission error in Phases 1, 2, and 3 depending on the number of cages used in each test (Fig. 7D–F). In Phase 1, the Kuskal–Wallis test indicated significant difference for both emulated frequencies, 5 Hz ($H_{(7)} = 53.960$; $p < 0.001$; $\eta^2 = 0.237$) and 10 Hz ($H_{(7)} = 52.764$; $p < 0.001$; $\eta^2 = 0.244$; Fig. 7D). For output B, Phase 2, the analysis detected significant differences for both emulated frequencies, 5 Hz ($H_{(7)} = 57.369$; $p < 0.001$; $\eta^2 = 0.380$) and 10 Hz ($H_{(7)} = 58.946$; $p < 0.001$; $\eta^2 = 0.530$; Fig. 7E). In Phase 3, considering both outputs, the analysis detected significant differences at 5 Hz ($H_{(7)} = 57.369$; $p < 0.001$; $\eta^2 = 0.405$) and at 10 Hz ($H_{(7)} = 58.946$; $p = 0.011$; $\eta^2 = 0.406$; Fig. 7F).

In vivo validation

In the final validation step, we recorded the drinking behavior of 48 mice for 12 nights in three sets containing eight cages with two lickometers in each cage (Fig. 8A). A positive correlation ($r = 0.81$, $p < 0.0001$, linear regression fitness $R^2 = 0.72$) was observed between the total amount of water or ethanol intake and lick counts acquired by our system. This correlation was also high if the type of liquid was considered (water: $r = 0.72$, $p < 0.0001$, linear regression fitness $R^2 = 0.73$; ethanol: $r = 0.79$, $p < 0.0001$, linear regression fitness $R^2 = 0.59$; Fig. 8C). In addition, Figure 8D shows an example trace of the acquired data, demonstrating the detailed microstructure and timestamps that can be collected by our device. Several microstructure parameters can be analyzed from the licks timestamps, for example: ILI, frequency, bouts, etc. in different time points of the experiments.

Discussion

Although the complexity of drinking behavior is of key importance in different types of studies, most labs still measure only the total volume drunk by animals, losing the detailed pattern of consumption. The microstructure can be easily measured with automatic lickometers (Barkley-Levenson and Crabbe, 2015; Cains et al., 2017; Frie and Khokhar, 2019; Godynyuk et al., 2019), but the commercially available ones are very expensive. In addition, the open-source options are designed for recording one animal per time. Thus, an extensive behavior protocol that demands several groups to be run together would cost a lot or demand great development efforts. We have developed and validated an automated lickometer device based on an open-source hardware platform with a user-friendly interface for monitoring measurements in real time. Among the advantages of our system, we highlight the extensive validation to show its reproducibility at an accessible low cost (the capital cost of one system, eight cages with two bottles each, was R\$10,000.00, real, Brazilian currency, which represents about \$2,000.00, in 2022). The device is easy to build and uses cheap components described in our GitHub webpage (https://github.com/kabrahao/BR_lickometer). Each house cage has two lickometers allowing researchers to offer two types of liquids to study preference and other variables. Each

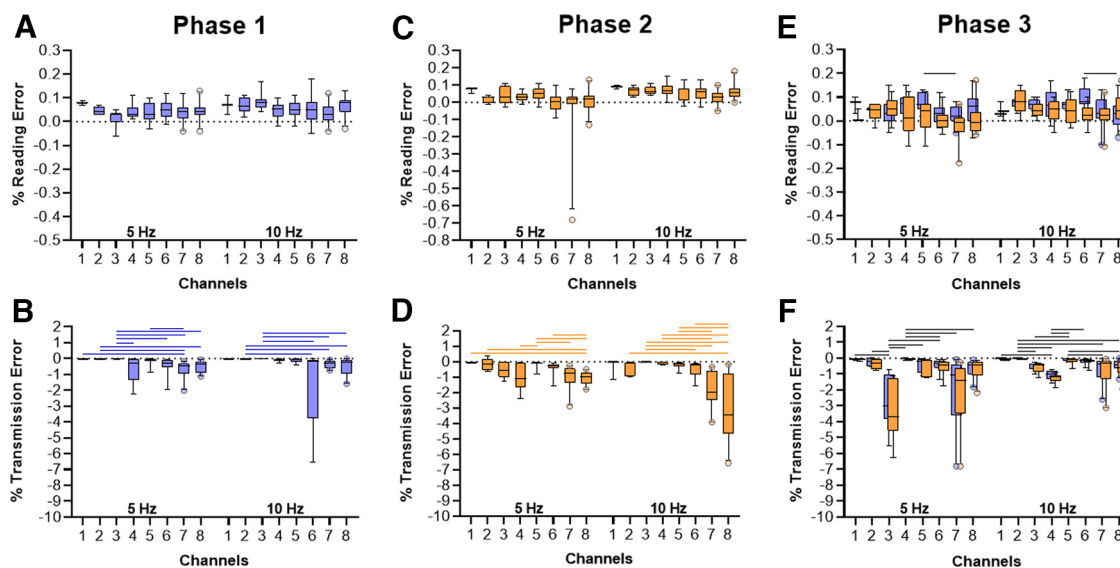


Figure 7. Results of reading and transmission errors obtained with the *in silico* validation of 5 and 10 Hz emulated frequencies for increasing number of cages (channels) receiving the signal (1–8). Box plots represent the mean and the whiskers 9th–95th percentile. Output A is represented in blue and output B is represented in orange. We describe the general range of the errors in this legend using mean \pm standard deviation. **A**, Reading error in Phase 1 (output A) at 5 Hz ranged around $0.0422 \pm 0.035\%$, and at 10 Hz, around $0.0559 \pm 0.0424\%$. **B**, Reading error in Phase 2 (output B) at 5 Hz ranged around $0.0173 \pm 0.0817\%$, and at 10 Hz, around $0.056 \pm 0.0415\%$. **C**, Reading error in Phase 3. Considering the 5-Hz frequency, output A shows a reading error ranging around $0.0466 \pm 0.0521\%$, and output B, around $0.0375 \pm 0.059\%$. At 10 Hz, output A shows a reading error ranging around $0.0594 \pm 0.054\%$, and output B, around $0.0679 \pm 0.0495\%$. **D**, Transmission error in Phase 1 (output A) at 5 Hz ranged around $-0.422 \pm 0.494\%$, and at 10 Hz, around $-0.484 \pm 1.073\%$. **E**, Transmission error in Phase 2 (output B) at 5 Hz ranged around $-0.661 \pm 0.61\%$, and at 10 Hz, around $-1.187 \pm 1.618\%$. **F**, Transmission error in Phase 3. Considering the 5-Hz frequency, output A shows a transmission error ranging around $-0.898 \pm 1.312\%$, and output B, around $-1.013 \pm 1.405\%$. At 10 Hz, output A shows a transmission error ranging around $-0.441 \pm 0.479\%$, and output B, around $-0.537 \pm 0.589\%$. Horizontal lines represent statistically significant differences of each error and each frequency in relation to the amount of channels, calculated by the Bonferroni *post hoc* analysis of an independent-samples Kruskal–Wallis test, $p < 0.05$.

complete device is able to successfully collect data from eight animals at the same time, allowing complex multi-group behavioral neuroscience studies to be performed.

Three validation steps were conducted to reach the final prototype and to guarantee its reliability in detecting licking events. First, we verified the most appropriate sensor for this application, according to the existing prototypes in the literature, which are mostly based on photoelectric (Frie and Khokhar, 2019; Godynyuk et al., 2019) or capacitive sensors (Longley et al., 2017). It is important to point out that these previous studies did not compare the sensors or checked the influence of different variables on their data. The capacitive sensor responded with greater precision and stability when compared with the photoelectric sensor. The results were independent of animal age and sex, and the experience of reviewers did not have an effect on the results. The electronic principles behind the prototype components may explain the efficiency difference. In the case of the photoelectric sensor, when the light beam is interrupted by an object, the current stops and the Arduino counts as a lick. However, if the mouse stops in front of the photograph emitter interrupting the beam without licking the bottle, the Arduino still counts a lick. Thus, the photoelectric prototype measures only the interest in the liquid rather than the actual licking behavior. The photometer sensor was used by Frie and Khokhar (2019) and Godynyuk et al. (2019). On the

other hand, the capacitive sensor works based on the electrical field between the 65-mm stainless steel nozzle and the ground platform. This system allowed the detection of a lick as a signal when the mouse touched the bottle nozzle with its tongue. Thus, our measurement is not only the interest in the liquid but the real licking behavior. It is important to point out that if the licking cabin is large, other parts of the mice's body may touch the nozzle and a spurious lick may be counted. To avoid these false positives, we restricted the cabin to allow only the approach of the mice snout.

The translation of the system to wireless allowed us to better monitor eight animals simultaneously, with two capacitive sensors per cage. In order to evaluate the prototype performance, we proposed the *in silico* validation step with simulated licks at extreme and typical rates. This step was important to verify the reading and transmission errors from the proposed system. Ideally, we expected no differences between the simulated conditions and phases of validation in the same frequencies, since the hardware requirements between phases would be similar. However, some statistical differences were found among different phases and different frequencies. Despite some differences in specific situations, the reading error mean was lower than 0.1% and the transmission error mean was lower than 10% in all tests. Transmission error though was higher for some validation phases probably because of

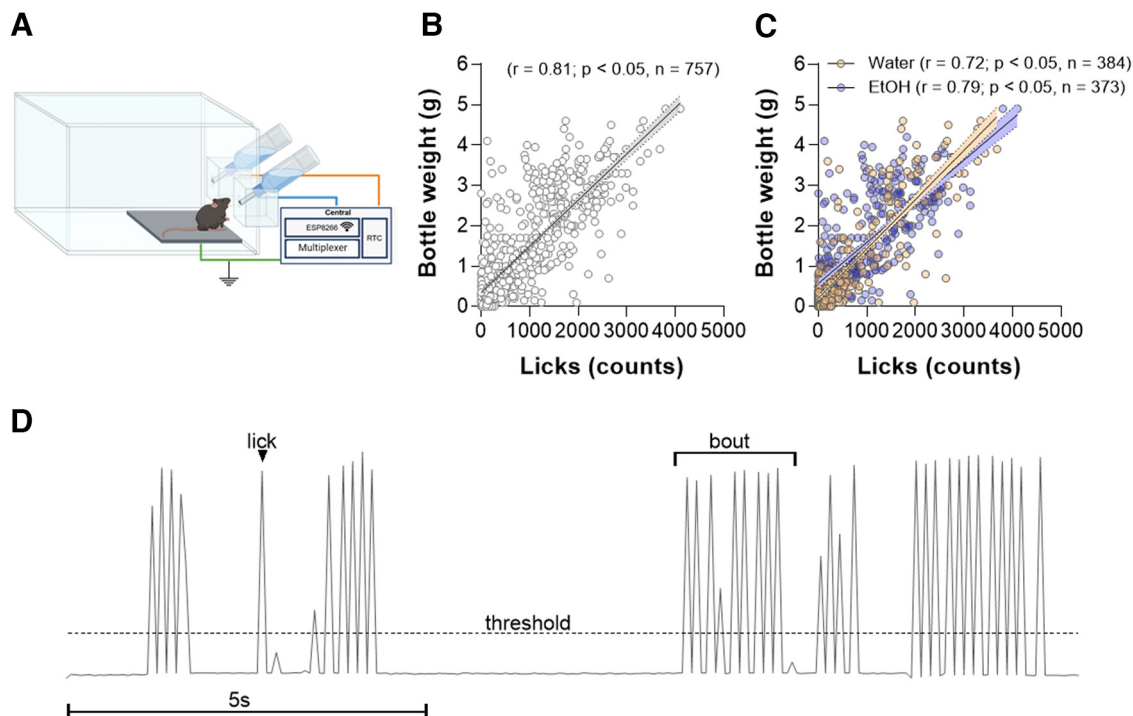


Figure 8. Results of the *in vivo* validation of the final lickometer system. **A**, Schematic representation of the one final cage containing two lickometers coupled to the central unit. **B**, Dispersion graph of the consumed liquid (difference of the bottle weight at the end of the experiment compared with the beginning of the experiment in grams - g) and total number of licks for each mouse in each session in the lickometer system. Spearman correlation revealed a strong correlation between the variables ($p < 0.05$). **C**, Dispersion graph of the consumed liquid (g) and total number of licks for each mouse in each session in the lickometer system separated by different types of liquids: water and 10% ethanol. Correlation analysis revealed strong correlation independently of the liquid presented to the animals ($p < 0.05$). **D**, Example trace of the raw acquired data demonstrating the detailed microstructure and time-stamp licks that can be collected by our device. High peaks indicate licks events.

busier network bandwidth during the simulation experiment. Thus, for wireless transmission prototypes, it is important to verify whether other wireless equipment is turned off to avoid loss of information. Thus, errors tend to be even lower in regular situations, guaranteeing a good performance of the system.

In the third part of our study, we collected simultaneous data from 24 cages that recorded the interaction of each animal with two bottles, over 12 sessions. For validation, we correlated the total amount of liquid consumed, measured by weighting the bottle before and after the test, with the lick count, obtaining a positive correlation. Previous studies used validation methods similar to ours. In general, validation usually involves the exposure of experimental animals to voluntary liquid consumption protocols, allowing the correlation of the consumed volume with the number of licks registered (Raymond et al., 2018; Godynyuk et al., 2019; Renteria et al., 2020). A similar validation method was adopted by Longley et al. (2017), who have developed a device with capacitive sensors and analyzed data from animals exposed to an operating protocol to obtain sucrose or water under a progressive reinforcement scheme.

Our data demonstrate that the device is useful in assessing the microstructure of consumption in behavioral studies. Another important contribution of the proposed system is the versatility of bottle volumes that could be

attached to the nozzle. To better accessibility of the mouse to the drinking cabin, we measured the best height and slope for the nozzle bottle to be ergonomic to the mouse features, considering cage and bottle support can influence licking behavior. Proper ergonomics reduce noise generated by the animal's own body, such as paws or tails activating the sensor. The lickometer acrylic cage dimensions are ideal for mice or young rats, but it is also relevant to mention that it could be easily adapted for rats by changing the dimensions of the acrylic cage. Additionally, the removable wall that supports the drinking sippers could be changed to one with higher positioning of the sippers for adult rats, and the top metal grid could be changed to a higher set allowing rats to show normal rearing behavior.

Some expertise is desirable to reproduce the construction of the apparatus. First, basic electronics circuit knowledge is necessary to build the printed circuit board. Developing the final wireless prototype requires an intermediate programming background to design the firmware that sends the sensor data to the computer wirelessly and the user interface that receives data in real time. We believe that researchers will be able to build the device in three months or less with the expertise mentioned before.

There are limitations in our system. The device does not measure volume, so there is no real-time information about the exact amount of volume consumed in each lick or bout, for example. Furthermore, manufacturing our lickometer

and installing the software requires knowledge beyond behavioral neuroscience, including software programming and hardware montage. Despite these limitations, the device is precise and valuable for drinking behavior measures at an accessible cost. In addition, the wireless adaptation allows the computer not to be necessary for the experimental room, reducing animal stress and changes in the light-dark cycle. In addition, the device has the potential to have data sent to the cloud, making it possible to monitor the experiment remotely and the potential to be coupled to *in vivo* neuroscience tools such as electrophysiological and photometrical neuronal recordings.

In conclusion, aiming to bring an innovative and low-cost solution for drinking behavioral studies, we proposed a lickometer system based on an open-source hardware platform with a user-friendly interface software, capable of simultaneously receiving data from eight automated cages with two drinking bottles each. Our results showed that the capacitive sensor presented appropriate recall and precision for this application. The device showed a reliable positive correlation between the total amount of liquid consumed and the licks count. Moreover, future work will involve adapting the system to send data to the cloud using the Internet network; algorithm improvements for creating an adaptive threshold; and system adaptation to include a volume sensor for automated measurement of consumed volume to enhance the study of licking microstructure.

References

- Bachmanov AA, Reed DR, Beauchamp GK, Tordoff MG (2002) Food intake, water intake, and drinking spout side preference of 28 mouse strains. *Behav Genet* 32:435–443.
- Bagder P (2015) Capacitive sensing library [www document]. Arduino. Available at <https://playground.arduino.cc/Main/CapacitiveSensor/>. Accessed December 14, 2021.
- Bainier C, Mateo M, Felder-Schmittbuhl MP, Mendoza J (2017) Circadian rhythms of hedonic drinking behavior in mice. *Neuroscience* 349:229–238.
- Barkley-Levenson A, Crabbe J (2015) Distinct ethanol drinking microstructures in two replicate lines of mice selected for drinking to intoxication. *Genes Brain Behav* 14:398–410.
- Boughter JD Jr, Baird JP, Bryant J, St. John SJ, Heck D (2007) C57BL/6J and DBA/2J mice vary in lick rate and ingestive microstructure. *Genes Brain Behav* 6:619–627.
- Cains S, Blomeley C, Kollo M, Rácz R, Burdakov D (2017) Agrp neuron activity is required for alcohol-induced overeating. *Nat Commun* 8:14014.
- Darevsky D, Hopf FW (2020) Behavioral indicators of succeeding and failing under higher-challenge compulsion-like alcohol drinking in rat. *Behav Brain Res* 393:112768.
- Darevsky D, Gill TM, Vitale KR, Hu B, Wegner SA, Hopf FW (2019) Drinking despite adversity: behavioral evidence for a head down and push strategy of conflict-resistant alcohol drinking in rats. *Addict Biol* 24:426–437.
- Eisenhardt M, Leixner S, Spanagel R, Bilbao A (2015) Quantification of alcohol drinking patterns in mice. *Addict Biol* 20:1001–1011.
- Frie JA, Khokhar JY (2019) An open source automated two-bottle choice test apparatus for rats. *HardwareX* 5:e00061.
- Gamsby JJ, Pribish AM, Stevanovic KD, Yunus A, Gullick D (2017) Alcohol intake long-light conditions. *Front Behav Neurosci* 11:152.
- Gero D, File B, Justiz J, Steinert RE, Frick L, Spector AC, Bueter M (2019) Drinking microstructure in humans: a proof of concept study of a novel drinkometer in healthy adults. *Appetite* 133:47–60.
- Godynuk E, Bluitt MN, Tooley JR, Kravitz AV, Creed MC (2019) An open-source, automated home-cage sipper device for monitoring liquid ingestive behavior in rodents. *eNeuro* 6:ENEURO.0292-19.2019.
- Jeanblanc J, Rolland B, Gierski F, Martinetti MP, Naassila M (2019) Animal models of binge drinking, current challenges to improve face validity. *Neurosci Biobehav Rev* 106:112–121.
- Longley M, Willis EL, Tay CX, Chen H (2017) An open source device for operant licking in rats. *PeerJ* 5:e2981.
- Panksepp JB, Rodriguez ED, Ryabinin AE (2017) Sweetened-ethanol drinking during social isolation: enhanced intake, resistance to genetic heterogeneity and the emergence of a distinctive drinking pattern in adolescent mice. *Genes Brain Behav* 16:369–383.
- Ramirez I, Sprott RL (1978) Hunger and satiety in genetically obese mice (C57BL/6J-ob/ob). *Physiol Behav* 20:257–264.
- Raymond M, Mast T, Breza J (2018) An open-source lickometer and microstructure analysis program. *HardwareX* 4:e00035.
- Renteria R, Cazares C, Gremel CM (2020) Habitual ethanol seeking and licking microstructure of enhanced ethanol self-administration in ethanol dependent mice. *Alcohol Clin Exp Res* 44:880–891.
- Rossi MA, Li HE, Lu D, Kim IH, Bartholomew RA, Gaidis E, Barter JW, Kim N, Cai MT, Soderling SH, Yin HH (2016) A GABAergic nigrotectal pathway for coordination of drinking behavior. *Nat Neurosci* 19:742–748.
- Williams B, Speed A, Haider B (2018) A novel device for real-time measurement and manipulation of licking behavior in head-fixed mice. *J Neurophysiol* 120:2975–2987.